LAMINAR CONVECTIVE COOLING OF DISCRETE HEATERS IN CHANNEL FLOW

Thiago Antonini Alves, antonini@fem.unicamp.br
Carlos A. C. Altemani, altemani@fem.unicamp.br
Unicamp – FEM – Departamento de Energia, Caixa Postal 6122, CEP: 13.083-970, Campinas, SP, Brasil

Abstract. *A numerical investigation was performed using the finite volumes method to evaluate the temperatures of three discrete strip heat sources flush mounted on a wall of a parallel plates channel. The upper and lower channel walls were adiabatic, except along the three strip heat sources, where a uniform heat flux was assumed at their surface. The heat sources were cooled under steady state conditions by a laminar airflow with constant properties forced into the channel considering either fully developed flow or a uniform velocity at the channel entrance. The solution of this thermal convection problem was presented in terms of a heat transfer coefficient, where three possibilities were employed for the reference temperature. The first was the fluid entrance temperature into the channel, the second was the flow mixed mean temperature just upstream any heater, and the third option employed the adiabatic temperature concept for each heater. It is shown that the last alternative gives rise to an invariant descriptor of the heat transfer, the adiabatic heat transfer coefficient, which depends solely on the flow and the heaters location. This is very convenient for the thermal analysis of electronic equipment, where the components' heating is discrete and can be highly non-uniform.*

Keywords*:* discrete heating, laminar channel flow, adiabatic heat transfer coefficient, numerical analysis.

1. INTRODUCTION

The convective heat transfer from an isothermal surface to a fluid flow is expressed through a simple definition of a heat transfer coefficient, as indicated in Eq. (1).

$$q = h_r A(T_w - T_r) \tag{1}$$

In this equation, q indicates the convective heat transfer rate and A represents the wetted surface area. T_w is the isothermal surface temperature and T_r is a fluid reference temperature. The choice of the reference temperature T_r in Eq. (1) defines the corresponding convective heat transfer coefficient h_r.

For uniform thermal boundary conditions, the reference temperature T_r may be conveniently chosen. In external flows, for example, it is equal to T_∞, the fluid free stream temperature far from the heat transfer surface, and the corresponding convective coefficient is h_∞. In internal flows, the reference is usually the local mixed mean fluid temperature T_m and the corresponding heat transfer coefficient is h_m, but sometimes the fluid inlet temperature T_{in} is also chosen as the reference, giving rise to h_{in}. Uniform boundary conditions and these reference temperatures usually lead to either a uniform or a monotonically varying convective heat transfer coefficient along the heat transfer surface.

There are however practical situations with non-uniform thermal boundary conditions in the flow direction. In these cases, the standard reference temperatures, like T_∞ in external flows and either T_m or T_{in} in internal flows, may lead to a very strange behavior of the corresponding heat transfer coefficient. A discontinuity in the wall temperature distribution, for example, may lead to a discontinuity of the local heat transfer coefficient from $-\infty$ to $+\infty$ (Kays and Crawford, 1993).

In electronics cooling, a typical circuit board may contain several discrete components, all dissipating electric power at distinct rates on their surfaces. The standard convective heat transfer coefficients based either on T_∞, T_m, or T_{in} may pose two main difficulties in this case. First, a step change on the board wall temperature from one component to the next may cause a discontinuity in the heat transfer coefficient from $-\infty$ to $+\infty$ along the board. Second, the electric power dissipation in the components could change, leading to distinct distributions of the heat transfer coefficient for each case. Worse, the values of these coefficients for any set of thermal boundary conditions on the circuit board would not be useful to the analysis of any additional proposed change.

These difficulties can be avoided if T_r in Eq. (1) is associated to the adiabatic surface temperature T_{ad} of any component on the circuit board. This is the temperature the component attains when its power dissipation rate is turned to zero while all the other components are dissipating power at their specified rates. Using T_{ad} as the reference temperature in Eq. (1), the adiabatic heat transfer coefficient h_{ad} is obtained. This concept was introduced by Arzivu and Moffat (1982) from experiments in electronics cooling and extended by subsequent works of Arzivu *et al.* (1985), Anderson and Moffat (1992a, 1992b), Moffat (1998) and Moffat (2004). They showed that the adiabatic heat transfer coefficient is an invariant descriptor of the convective heat transfer. It is independent of the thermal boundary conditions, being a function only of the geometry and flow characteristics - a brief description, based on these works, will be presented in section 2.

There are several works presented in the literature related to the convective heat transfer from either a single heater or an array of heat sources which are flush mounted to one wall of a channel or of a rectangular duct. Incropera *et al.* (1986) performed experiments to determine the Nusselt number from a single heat source and from an in-line array of 12 heat sources distributed in four rows, with three heaters per row. All heaters were made from copper blocks flush mounted to one wall of a rectangular duct and the array data were obtained running the experiments with the same power input to all the heaters. They also presented results of two-dimensional simulations and compared the predictions with the experimental data, mostly in the turbulent flow regime. Their heat transfer coefficient for each heater was defined using the flow inlet temperature as the reference in Eq. (1). Mahaney *et al.* (1990) also presented experimental data from a similar array of 12 heaters distributed in four rows, with three heaters per row. Their data were obtained under mixed laminar convection and compared with three dimensional numerical simulations. The array was mounted to the lower horizontal wall of a rectangular duct and the heaters were also made from copper blocks. The heat transfer coefficient for any heater was defined using the mixed mean fluid temperature just upstream the heater, as the reference in Eq. (1). Sugavanam *et al.* (1995) performed a numerical simulation of the conjugate effects of substrate conduction and forced convection air-cooling of a uniformly powered strip source flush mounted to a wall of a parallel-plate channel. They defined the convective heat transfer coefficient using the channel flow inlet temperature as the reference in Eq. (1). Ortega and Lall (1992) considered a small strip heat source (q_s") flush mounted to one wall of a parallel-plate channel. The wall thermal boundary condition was either adiabatic (q_w" = 0) or a uniform heat flux (q_w" < q_s") downstream and upstream the heat source. They investigated numerically the effect of the heat source position along the channel length on the average Nusselt number over the heat source. The analysis was performed under conditions of laminar developing flow and also fully developed flow at the channel entrance. The Nusselt number was defined using the local mixed mean temperature (T_m) and also the adiabatic temperature (T_{ad}) as the reference. For fully developed flow at the channel entrance, the average Nu_m over the heat source was independent of the heat source position when the upstream wall was adiabatic. When the upstream wall was heated, the source average Nu_m decreased along the channel length. On the other hand, for the same flow and thermal conditions, the heat source average value of Nu_{ad} was uniform along the channel length, independently of the upstream wall thermal conditions. Moffat (1998) presented the quest for invariant descriptors of the convective process which can deal with non-uniform thermal boundary conditions. He presented a historical review of the heat transfer coefficient, with emphasis on h_{ad} and T_{ad} and described some difficulties in measuring these quantities. Experimental results for the heat transfer coefficient on heated blocks in a channel were presented and it was shown that the related measurement of T_{ad} should be made very accurately else the derived coefficients would be useless.

In the present work, three distinct heat transfer coefficients, defined for the reference temperatures T_{in}, T_m and T_{ad}, were obtained from numerical simulations for the configuration indicated in Fig. 1. Three strip heaters flush mounted to a wall of a parallel plate channel were cooled by a forced flow in the laminar regime. Two distinct flow conditions were investigated – a fully developed flow at the channel inlet and a developing flow starting with a uniform velocity profile at the channel inlet. Each heater had the same length L_h and the spacing from one heater to another was L_s. Their position in the channel was defined by the upstream length L_u and the downstream length L_d. The simulations were performed considering $L_u = 5\ L_c$, $L_d = 10\ L_c$ and under the conditions of $L_h = L_s = L_c$, the total channel length was equal to $L = 20\ L_c$, where L_c is the channel height, as indicated in Fig. 1.

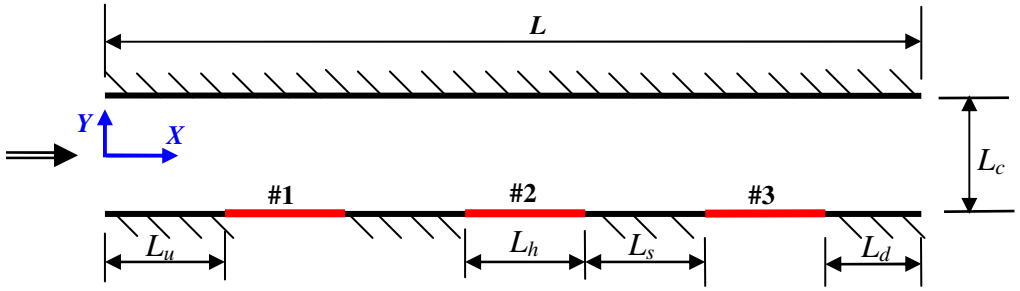

Figure 1. Three heaters flush mounted to a channel wall.

2. ANALYSIS

2.1. The adiabatic heat transfer coefficient

Considering an array of flush mounted heaters to a channel wall, as indicated in Fig. 1, the adiabatic heat transfer coefficient for any heater is most easily obtained when only the n^{th} component of the array is heated and all the others are kept inactive. Under these conditions, the fluid inlet temperature in the channel is also the adiabatic wall temperature of the active component. For a particular flow condition, the convective heat transfer rate is proportional to the difference $(T_w - T_{ad})_n$ and Eq. (1) gives the adiabatic heat transfer coefficient $h_{ad,n}$. The active heater temperature rise above its adiabatic temperature is due solely to self-heating in this case. The convective heat q_n released by the n^{th} component of the array causes a mixed mean flow temperature rise $(\Delta T_m)_n$ obtained by an energy balance.

$$(\Delta T_m)_n = \frac{q_n}{\dot{m}\, c_p} \tag{2}$$

Using a procedure similar to that of Anderson and Moffat (1992,b) for a two-dimensional array, the temperature differences $(T_w - T_{ad})_n$ and $(\Delta T_m)_n$ can be related, for the linear array indicated in Fig. 1, by the definition of an influence coefficient $g^*(n–n)$.

$$(T_w - T_{ad})_n = (\Delta T_m)_n \; g^*(n-n) = \frac{q_n}{\dot{m} c_p} g^*(n-n) \tag{3}$$

When two or more heaters are simultaneously active, the temperature rise of any heater above the channel inlet flow temperature is due to both its self-heating and the thermal wake effect from the upstream active heaters. The thermal wake increases the adiabatic temperature of all downstream heaters above the inlet fluid temperature T_{in}. These two effects can be expressed by the following equation.

$$(T_w - T_{in})_n = (T_w - T_{ad})_n + (T_{ad} - T_{in})_n \tag{4}$$

If the fluid flow were completely mixed, the adiabatic temperature rise of a component would be equal to the mixed mean temperature rise due to all upstream components. Due to imperfect mixing, the mixed mean temperature rise is always lower than the adiabatic temperature rise of any component. This effect can also be expressed by a relation between the adiabatic and the mixed mean temperature rises of the n^{th} row component of the linear array indicated in Fig. 1. For each active component in the i^{th} row of the array, upstream the n^{th} component, an influence coefficient $g^*(n\text{-}i)$ is defined by

$$(T_{ad} - T_{in})_{n-i} = (\Delta T_m)_i \; g^*(n-i) = \frac{q_i}{\dot{m} c_p} g^*(n-i) \tag{5}$$

Considering all the active components upstream the n^{th} row of the linear array, and making use of both influence coefficients, Eq. (4) can be rearranged as

$$(T_w - T_{in})_n = \frac{q_n}{\dot{m} c_p} g^*(n-n) + \sum_i \frac{q_i}{\dot{m} c_p} g^*(n-i) \tag{6}$$

From Equations (3) and (6), expressions for h_{ad} and h_{in} can be obtained as follows.

$$h_{ad,n} = \frac{q''_n}{(T_w - T_{ad})_n} = \frac{\dot{m} c_p}{A_n \, g^*(n-n)} \tag{7}$$

$$h_{in,n} = \frac{q''_n}{(T_w - T_{in})_n} = \frac{q''_n}{\frac{q_n}{\dot{m} c_p} g^*(n-n) + \sum_i \frac{q_i}{\dot{m} c_p} g^*(n-i)} \tag{8}$$

As indicated by Moffat (1998), there are no thermal boundary conditions in Eq. (7), i.e., h_{ad} is a function of flow parameters only. For the same geometry and flow conditions, the value of h_{ad} obtained by any type of test will be the same for any other thermal conditions. Thus, in a convective cooled circuit board populated with several components, the value of h_{ad} for any component will not depend on the distribution of electric power dissipation. Comparatively, the correlation for h_{in} is much more complex, involving the heat flow from each component on the board. In Equation (8), the value of h_{in} will be the same for any level of heating only when all the components dissipate heat at the same rate.

2.2. Problem formulation and heat transfer parameters

The flow in the channel depicted in Fig. 1 was considered in the laminar regime under steady state conditions and constant fluid properties. The velocity and temperature profiles were obtained by numerical simulations using the control volumes method (Patankar, 1980) and the SIMPLE (Semi-Implicit Method for Pressure Linked Equations) algorithm.

When the flow was assumed developed at the channel entrance, the velocity profile was taken from the analytical solution with a parabolic profile and the numerical simulations were needed only for the temperature distribution. In this case, the velocity component normal to the plates (v) was zero and that along the plates (u) was

$$u(y) = \frac{3}{2}\bar{u}\left(1 - \frac{4y^2}{L_c^2}\right) \tag{9}$$

A Reynolds number was defined, using the channel hydraulic diameter, as

$$Re = \frac{\bar{u} \; 2L_c}{\nu} \tag{10}$$

Three values of Reynolds were employed in the numerical simulations: 630, 1260 and 1890. For L_c = 1 cm and considering that the fluid is air at 300 K, these values correspond to average velocities along the channel respectively close to 0,5 m/s, 1 m/s and 1,5 m/s.

When the velocity profile was considered uniform at the channel entrance, then the simultaneous development of the velocity and the temperature profiles were obtained from the numerical solution of the conservation equations of mass, momentum and energy. These equations were expressed in dimensionless form as follows.

$$\frac{\partial U}{\partial X}+\frac{\partial V}{\partial Y}=0 \tag{11}$$

$$U\frac{\partial U}{\partial X}+V\frac{\partial U}{\partial Y}=-\frac{\partial P^*}{\partial X}+\left(\frac{\partial^2 U}{\partial X^2}+\frac{\partial^2 U}{\partial Y^2}\right) \tag{12}$$

$$U\frac{\partial V}{\partial X}+V\frac{\partial V}{\partial Y}=-\frac{\partial P^*}{\partial Y}+\left(\frac{\partial^2 V}{\partial X^2}+\frac{\partial^2 V}{\partial Y^2}\right) \tag{13}$$

$$U\frac{\partial \theta}{\partial X}+V\frac{\partial \theta}{\partial Y}=\frac{1}{Pr}\left(\frac{\partial^2 \theta}{\partial X^2}+\frac{\partial^2 \theta}{\partial Y^2}\right) \tag{14}$$

The dimensionless variables used in the conservation equations were defined by

$$X=\frac{x}{L},\quad Y=\frac{y}{L},\quad U=\frac{\rho u L}{\mu},\quad V=\frac{\rho v L}{\mu},\quad P^*=\frac{P\rho L^2}{\mu^2},\quad \theta=\frac{T-T_{in}}{\left(\frac{q_s'' L_h}{k}\right)} \tag{15}$$

The boundary conditions for the developing flow encompassed a uniform velocity at the channel entrance and the no-slip condition at the channel walls. The thermal boundary conditions were a uniform temperature at the channel inlet, equal to T_{in}, and an adiabatic condition at the channel walls, except along any active heater, where a uniform heat flux was considered.

The temperature field obtained from the numerical simulations was employed to evaluate the average heat transfer coefficient for any active heater. In the revised literature, the experimental tests were performed with isothermal heated blocks made from copper or aluminum. In the present analysis, the heaters were flush mounted to a channel wall and released a uniform heat flux, so that their surface was not isothermal. In this case, the convective coefficient for the n^{th} heater was based on the difference of its average surface temperature and the chosen reference temperature T_r (either T_{in}, T_m, or T_{ad}).

$$\bar{h}_{r,n}=\frac{q_n''}{\overline{T}_{h,n}-T_{r,n}},\qquad where\qquad \overline{T}_{h,n}=\frac{1}{L_h}\int_{L_h} T_{h,n}(x)\,dx \tag{16}$$

When T_{in} was chosen as the reference temperature, it is evident from Eq. (15) that $(\theta_r)_{in} = 0$.

When the selected reference was the mixed mean T_m, it was evaluated numerically at the upstream end of the considered active heater. For constant fluid properties, it was obtained from

$$T_{m,n}=\frac{\int_{A_c} uT dA}{\int_{A_c} u dA}\qquad and\qquad (\theta_r)_{m,n}=\frac{T_{m,n}-T_{in}}{\left(\frac{q'' L_h}{k}\right)} \tag{17}$$

When the adiabatic temperature T_{ad} was chosen as the reference, its value was obtained from the average heater surface temperature when its power was turned off and there were other active upstream heaters.

$$\overline{T}_{ad,n}=\frac{1}{L_h}\int_{L_h} T_{ad,n}(x)dx\qquad and\qquad (\theta_r)_{ad,n}=\frac{\overline{T}_{ad,n}-T_{in}}{\left(\frac{q'' L_h}{k}\right)} \tag{18}$$

The heater length L_h was chosen the characteristic length for the average Nusselt number, due to the thermal boundary layer nature of the heat transfer from the small heaters. Using the heat transfer coefficient defined in Eq. (16), the average Nu for the n^{th} heater in the array was expressed by

$$\overline{Nu}_{r,n}=\frac{\bar{h}_{r,n} L_h}{k}=\frac{1}{\bar{\theta}_{w,n}-\theta_{r,n}} \tag{19}$$

The easiest way to find the adiabatic heat transfer coefficient is to consider only a single active heater in the channel. Under this condition, the fluid inlet temperature and its mixed mean temperature upstream the single active heater are also the adiabatic surface temperature, all equal to T_{in}. The corresponding average Nusselt number is also the same for the three considered reference temperatures. The initial simulations were performed to evaluate the average Nu for a single active heater in the channel.

Additional simulations were performed next considering two or three active heaters in the channel, to obtain the influence coefficients $g^*(n–n)$ and $g^*(n–i)$, as defined by Eqs. (3) and (5). The purpose of these coefficients is to

predict the average temperature of each active heater, as indicated by Eq. (6). With two or more active heaters in the channel, the heat flux may be distinct from heater to heater. In this case, the smallest heat flux was the adopted value of q_s" used in the definition of the dimensionless temperature θ, and the corresponding Nusselt number for the n^{th} heater was expressed by

$$\overline{Nu}_{r,n} = \left(\frac{q''_n}{q''_s}\right)\frac{1}{\bar{\theta}_{w,n} - \theta_{r,n}} \tag{20}$$

For three active heaters in the channel, the distinct average Nusselt numbers, considering the three reference temperatures, were evaluated and compared. In addition, the numerical values of the average heaters temperatures were compared with the predictions based on Eq. (6), using the heat flux from each heater and the influence coefficients $g^*(n–i)$ obtained from the previous simulations.

2.3. Numerical simulation

The set of conservation equations (11) to (14) were solved within the domain shown in Fig. 1, with the indicated boundary conditions. The equations were solved by the control volumes method and the SIMPLE algorithm was used to obtain the velocity field. The relative dimensions employed in the simulations, according to the geometry specified in Fig. 1 were $L_u = 5\ L_c$, $L_d = 10\ L_c$ and $L_h = L_s = L_c$, so that the total channel length was $L = 20\ L_c$. A non-uniform grid was used in both the x and the y directions of the domain. In the x-direction, the grid was concentrated on the heaters surface – numerical tests using 20 to 100 uniformly distributed nodes on each heater indicated a convergence with 60 nodes. The grid deployment on the upstream length L_u, the spacing L_s between the heaters and the downstream length L_d was also tested numerically. The number of grid points selected for these three regions were respectively equal to 16, 11 and 26 and any further grid refinement did not change the numerical results. In the y-direction, tests were performed with both a uniform and a non-uniform grid. For the uniform grid in the y-direction, numerical tests were performed varying the number of grid points from 10 to 80, and the results converged for 60 control volumes. For the non-uniform grid, the smallest control volumes were near the walls of the channel, and their size increased by a geometric ratio towards the mid-plane between the channel walls. Numerical tests were performed with the non-uniform grid ranging from 10 to 40 grid points and the results converged for 20 control volumes. Due to its convergence with a significantly smaller number of grid points, the non-uniform grid in the y-direction was adopted to obtain the numerical results. The computations were performed in a microcomputer with a Pentium 4 HT processor 3.06GHz with 512MB RAM and a typical solution for a particular case demanded about 3 (three) minutes.

3. RESULTS

All the simulations were performed for a fluid with $Pr = 0.7$ (air) and three values of the channel Reynolds number, as defined by Eq. (10), in the laminar regime (630, 1260 and 1890).

3.1. A single active heater

The initial simulations with a single active heater in the channel were performed to obtain the average Nu_{ad} distributions for each heater. As mentioned before, the values of Nu_{in} and of Nu_m are the same as Nu_{ad} in this case, due to the coincidence of the reference temperatures. When the flow was fully developed at the channel entrance, the average Nu_{ad} values were independent of the heater position but changed with the Reynolds number, as indicated in Table 1.

Table 1. Average Nusselt for the heaters under fully developed channel flow conditions.

Re	$\boldsymbol{Nu_{ad} = Nu_{in} = Nu_m}$
630	9.31
1260	11.79
1890	13.55

When the flow was uniform at the channel entrance, its development was distinct along each heater in the channel. Thus, the average Nusselt over each heater depended also on its position in the channel. Considering again a single active heater in the channel, the average Nu values were also independent of the three reference temperatures, due to their coincidence. Table 2 presents the average Nusselt for each heater in this case, indicating the Reynolds and position dependence. Due to the simultaneous thermal and velocity boundary layer development over the heaters, the values indicated in Table 2 are always higher than those for the developed flow at the same Reynolds, as indicated in Table 1. In addition, the velocity boundary layer development in the channel also implies the higher values for the upstream heaters. These results are also presented in Fig. 2, where a line was drawn linking the calculated results for the three values of Re, just to distinguish better one case from the other. It is noticed the coincidence of the results for the three heaters when the flow is fully developed from the channel entrance, and their distribution when the flow is developing along the channel.

Table 2. Average Nusselt distributions under developing channel flow conditions.

Re	Nu_1	Nu_2	Nu_3
630	9.74	9.58	9.47
1260	12.93	12.62	12.42
1890	15.36	14.94	14.65

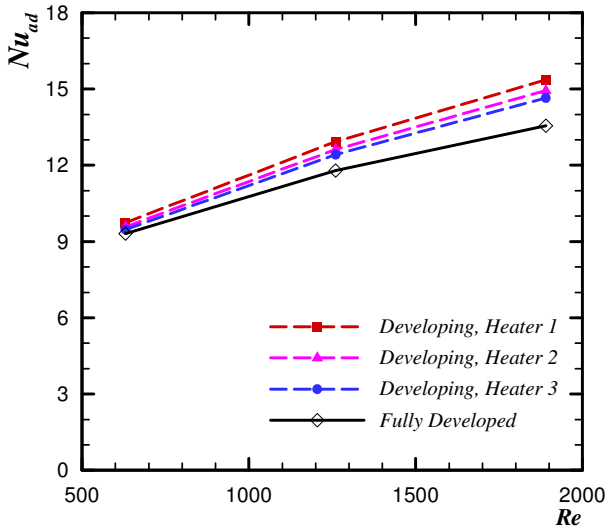

Figure 2. Average values of Nu_{ad} for fully developed and for developing channel flow (Pr = 0.7)

Another parameter obtained from the simulations with a single active heater was the influence coefficient $g^*(n–n)$, as defined in Eq.(3), due to self-heating of any heater. When the flow was fully developed from the channel entrance, it had the same velocity profile over any heater and the coefficient $g^*(n–n)$ was independent of the heater position – it changed only with the Reynolds number. The results (corresponding to Pr = 0.7) are indicated as $g^*(0)$ in Table 3. The values increase with *Re*, mainly due to an increased mass flow rate in the channel. For the case of developing flow, the influence of *Re* on the coefficients $g^*(n–n)$ presented the same trend with the change of Re. In addition, these coefficients also depended on the heater position, increasing downstream mainly due to the velocity boundary layer development and a higher heater mean temperature. These results are presented in Table 3, as $g^*(1–1)$, $g^*(2–2)$ and $g^*(3–3)$.

Table 3. Fully developed and developing channel flow values of $g^*(n–n)$.

Re	*Developed*	*Developing flow*		
	$g^*(0)$	$g^*(1\text{-}1)$	$g^*(2\text{-}2)$	$g^*(3\text{-}3)$
630	23.6842	22.6386	23.0167	23.2841
1260	37.4046	34.1067	34.9445	35.5072
1890	48.8192	43.0664	44.2771	45.1536

3.2. Two or three active heaters

These simulations were performed initially with two active heaters dissipating the same heat flux. Again, the flow was considered either fully developed or with a uniform profile at the channel entrance, for the same Reynolds numbers employed with a single active heater. The main purpose of these tests was to obtain the influence coefficients $g^*(n–i)$, as defined in Eq. (5). For fully developed channel flow, the coefficients $g^*(2–1)$ and $g^*(3–2)$ depended only on the channel Reynolds number and they were equal, due to the adopted geometry with the same heater length L_h and spacing L_s. They are represented by $g^*(1)$ in Table 4. The coefficient $g^*(3–1)$ indicates the adiabatic temperature rise of heater 3 above the channel flow inlet temperature due to the heat flux on heater 1 and it is indicated as $g^*(2)$ in Table 4. Again, these coefficients increase with *Re* due to a larger flow rate and the values of $g^*(1)$ are larger than those of $g^*(2)$ because the former represent the influence of a closer upstream heater. For a developing flow from a uniform profile at the channel inlet, these coefficients depended on the heater position, due to the flow development. They increased downstream mainly due to the velocity boundary layer development and in the limit of a far downstream position, they would equal the values attained for the fully developed flow, indicated by $g^*(1)$ and $g^*(2)$. The values of Nu_{ad} obtained from these simulations were identical to those presented in Tables 1 and 2, respectively for the fully developed and for the developing channel flow.

Table 4. Fully developed and developing channel flow values of $g^*(n–i)$.

Re	*Developed flow*		*Developing flow*		
	$g^*(1)$	$g^*(2)$	$g^*(2\text{-}1)$	$g^*(3\text{-}2)$	$g^*(3\text{-}1)$
630	7.2078	4.5398	7.0595	7.1229	4.4769
1260	11.2818	7.0482	10.6108	10.7978	6.7406
1890	14.6848	9.1282	13.4057	13.6538	8.4941

The simulations involving three active heaters included one case with the same heat flux on the heaters and two cases with distinct heat fluxes. Considering the heaters indicated in Fig. 1, the heat flux distribution in the first case was $q_1" = q_2" = q_3"$, corresponding to a heat flux ratio equal to 1-1-1 (case 1) for the three heaters. For the other two cases, with distinct heat fluxes, the corresponding ratios were equal to 5-3-1 (case 2) and to 3-5-1 (case 3).

Under fully developed channel flow, the numerical results for the average Nusselt numbers are presented in Table 5. The average Nu_{ad}, based on the adiabatic surface temperature, was invariant with the changes of the thermal conditions and, as expected, the values are the same as those shown before in Table 1. These values change only with the Reynolds number, as indicated in Fig. 2. For the heater in the first row (#1) the values of Nu_m and Nu_{in} are also the same as Nu_{ad}, again due to the coincidence of the reference temperatures. For the downstream rows (#2 and #3), the values of Nu_m and Nu_{in} change with the thermal conditions, as indicated in Table 5. Thus, it is evident the advantage and convenience to use Nu_{ad}. It is an invariant descriptor of the convective heat transfer, independent of the thermal boundary conditions, and can be obtained under much simpler conditions, as that with a single active heater in the channel. The results of Table 5 for the heater #3 are also presented in Fig. 3, showing the changes of Nu_{ad}, Nu_m and Nu_{in} for the three cases considered in the simulations. Since these values were obtained under fully developed channel flow, the values of Nu_{ad} were identical for the three heaters.

For the developing channel flow, the average Nusselt numbers are indicated in Table 6. The Nu_{ad} values are the same as those presented in Table 2, indicating again the invariant nature of this parameter as a descriptor of the convective heat transfer. The values of the other two Nu definitions change with the thermal conditions, as can be observed in Table 6. The values for the first row (heater #1) are the same as those of Nu_{ad} due to the mentioned coincidence of the reference temperatures for his row. The values presented in Table 6 for the heater #3 are shown also in Fig. 4, indicating again the invariant description of the convective heat transfer made by Nu_{ad}, while the values associated to the other definitions change with the thermal boundary conditions.

The heaters average wall temperature above the channel inlet flow temperature, as predicted by Eq. (6), was expressed in dimensionless form by the following equation, where $q_s"$ indicates the heaters smallest heat flux, used as the reference in defining the dimensionless temperature θ in Eq. (15). The influence coefficients g^* were those presented in Tables 3 and 4.

$$\bar{\theta}_n = \frac{2\,(q_n"/q_s")}{Re\,Pr}\,g^*(n-n) + \sum_i \frac{2\,(q_i"/q_s")}{Re\,Pr}\,g^*(n-i) \tag{21}$$

The numerical values for the average heaters temperatures obtained from the simulations for the three considered cases were compared with the predictions of Eq. (21). The results for the heater #3 are presented in Table 7, under conditions of fully developed and developing channel flow. For the three cases considered with three active heaters, the agreement was always within 0.1 %. For each case the value of θ decreases with Re, as indicated by Eq. (21). In each case, due to the higher values of the influence coefficients g^* indicated in Tables 3 and 4, the values of θ for the fully developed channel flow are higher than those for the developing flow.

Table 5. Average Nusselt numbers for the fully developed channel flow.

Re	*Heater*	*Case 1: ratio 1-1-1*		*Case 2: ratio 5-3-1*		*Case 3: ratio 3-5-1*		*All cases*
		Nu_m	Nu_{in}	Nu_m	Nu_{in}	Nu_m	Nu_{in}	Nu_{ad}
630	**1**	9.31	9.31	9.31	9.31	9.31	9.31	9.31
	2	7.38	7.14	6.48	6.18	8.05	7.88	9.31
	3	6.60	6.22	3.67	3.24	3.37	3.01	9.31
1260	**1**	11.79	11.79	11.79	11.79	11.79	11.79	11.79
	2	9.25	9.06	8.08	7.84	10.12	9.98	11.79
	3	8.21	7.91	4.48	4.14	4.12	3.83	11.79
1890	**1**	13.55	13.55	13.55	13.55	13.55	13.55	13.55
	2	10.59	10.42	9.24	9.03	11.60	11.48	13.55
	3	9.36	9.11	5.07	4.77	4.67	4.42	13.55

The numerical values of the dimensionless temperature distributions on each heater surface for case 2 (heat flux ratios 5-3-1) under fully developed channel flow are presented in Fig. 5, together with the corresponding adiabatic distributions. They indicate the expected increase of the heaters temperature along the flow and the corresponding decrease of their adiabatic surface temperature. The average temperatures obtained for each heater and employed in the definition of the adiabatic heat transfer coefficient are also indicated in Fig. 5. It should be noted that the adiabatic surface temperature for heater # 1 is coincident with T_{in}, so that its dimensionless temperature, as defined by Eq. (18) is equal to zero.

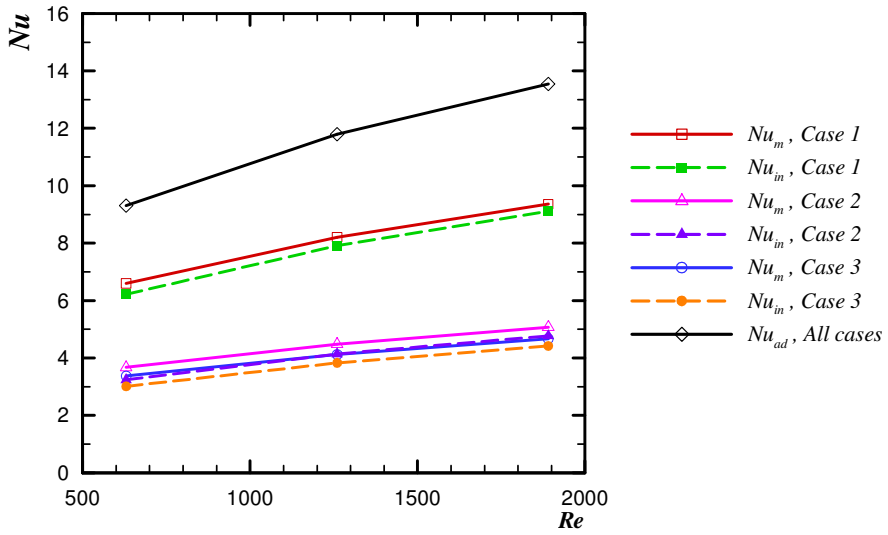

Figure 3. Three cases of the average Nusselt for heater #3 under fully developed channel flow.

Table 6. Average Nusselt numbers for the developing channel flow.

Re	*Heater*	*Case 1: ratio 1-1-1*		*Case 2: ratio 5-3-1*		*Case 3: ratio 3-5-1*		*All cases*
		Nu_m	Nu_{in}	Nu_m	Nu_{in}	Nu_m	Nu_{in}	Nu_{ad}
630	**1**	9.74	9.74	9.74	9.74	9.74	9.74	9.74
	2	7.59	7.33	6.67	6.34	8.28	8.09	9.58
	3	6.71	6.33	3.74	3.29	3.43	3.05	9.47
1260	**1**	12.93	12.93	12.93	12.93	12.93	12.93	12.93
	2	9.90	9.69	8.66	8.38	10.84	10.68	12.62
	3	8.65	8.32	4.72	4.35	4.34	4.03	12.42
1890	**1**	15.36	15.36	15.36	15.36	15.36	15.36	15.36
	2	11.67	11.47	10.19	9.93	12.79	12.64	14.94
	3	10.13	9.83	5.49	5.15	5.06	4.76	14.65

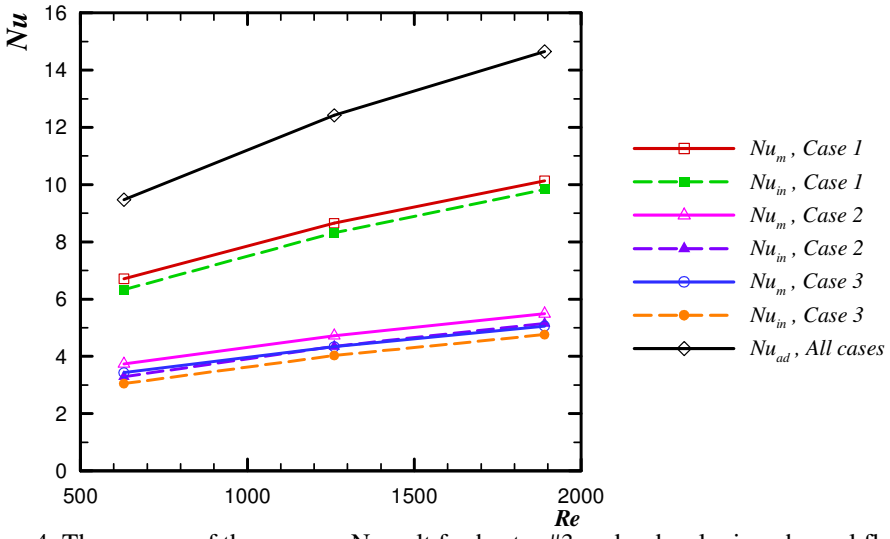

Figure 4. Three cases of the average Nusselt for heater #3 under developing channel flow.

Table 7. Numerical results and predictions for heater #3 average dimensionless temperature.

Re	*Developing Flow*					
	Case 1		*Case 2*		*Case 3*	
	$\theta_{3\ pred.}$	$\theta_{3\ numer.}$	$\theta_{3\ pred.}$	$\theta_{3\ numer.}$	$\theta_{3\ pred.}$	$\theta_{3\ numer.}$
630	0.1582	0.1581	0.3040	0.3040	0.3280	0.3279
1260	0.1203	0.1203	0.2304	0.2302	0.2488	0.2485
1890	0.1017	0.1017	0.1944	0.1944	0.2100	0.2100
Developed Flow						
630	0.1607	0.1608	0.3084	0.3086	0.3326	0.3328
1260	0.1264	0.1264	0.2415	0.2415	0.2607	0.2609
1890	0.1098	0.1098	0.2094	0.2096	0.2262	0.2264

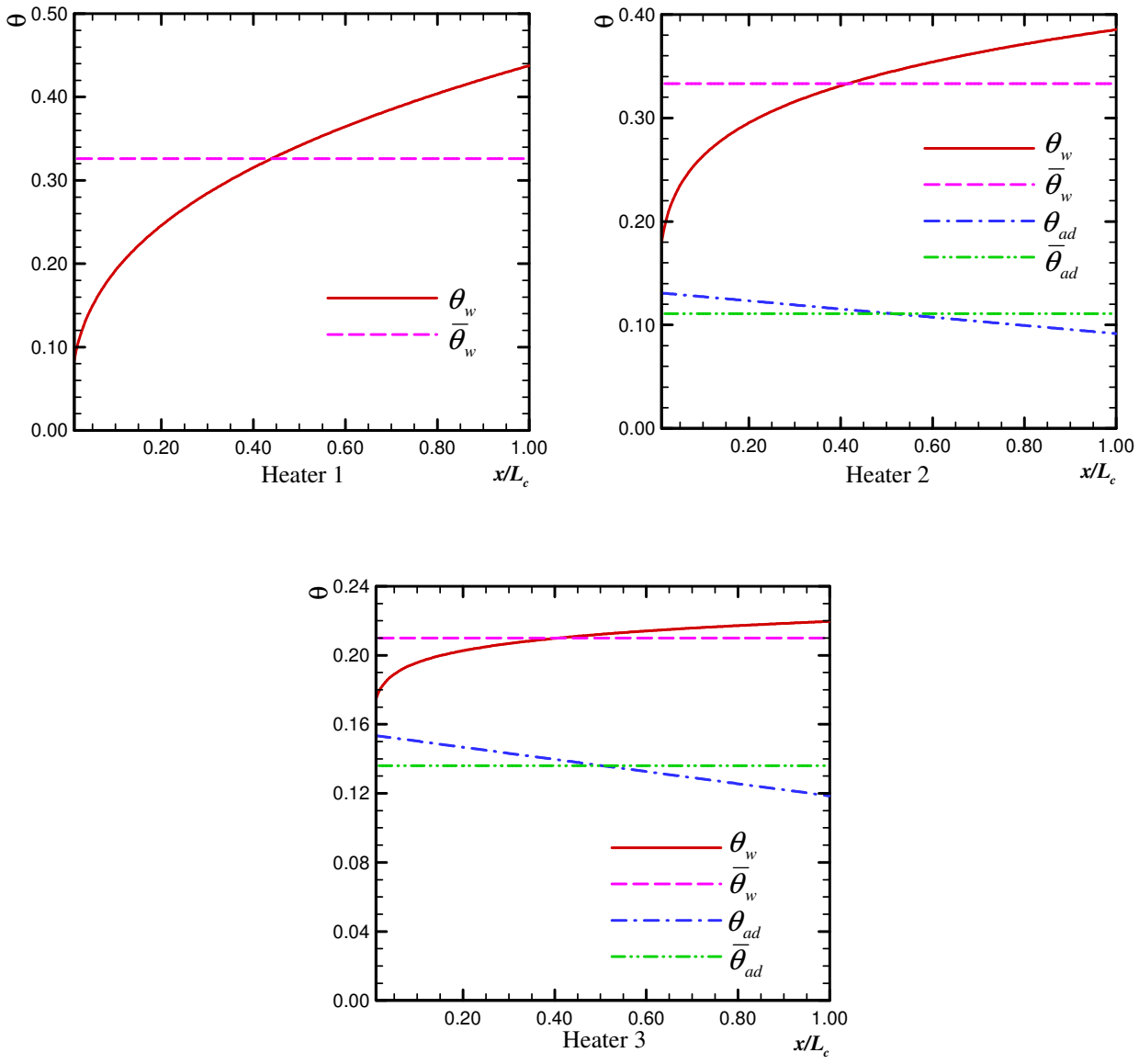

Figure 5. Dimensionless temperature distribution for all heaters in case 2 under fully developed channel flow.

4. CONCLUSIONS

Numerical simulations of the laminar convective heat transfer from three discrete heaters flush mounted to a single wall of a channel showed that the average Nu_{ad} for each heater is independent of their heat flux distribution. Comparatively, the evaluated average values of Nu_m and Nu_{in} are dependent on the heat flux distribution. This result is quite important, because the Nu_{ad} predictions can then be made under much simpler conditions, like a single active heater in the channel and the results can be applied to any other thermal condition of the three heaters. In addition, it was shown that the heaters' average temperature distributions under any thermal conditions can be predicted using influence coefficients g^* and the superposition principle since the energy equation is linear. These coefficients can be obtained from simulations with a single active heater and with two active heaters having the same heat flux. The resulting values can then be applied to predict the average heaters temperatures for any other thermal conditions with three active heaters. The present work was performed with three heater rows, but the method can be extended to a larger number of rows.

5. ACKNOWLEDGEMENTS

The support of CNPq (Brazilian Research Council) for the first author in the form of a doctorate program scholarship is gratefully acknowledged.

6. REFERENCES

Anderson, A. and Moffat, R.J., 1992a, "The Adiabatic Heat Transfer Coefficient and the Superposition Kernel Function: Part I – Data for Array of Flatpack for Different Flow Conditions", Journal of Electronics Packaging, Vol. 114, pp. 14-21.

Anderson, A. and Moffat, R.J., 1992b, "The Adiabatic Heat Transfer Coefficient and the Superposition Kernel Function: Part II – Modeling Flatpack Data as a Function of Turbulence", Journal of Electronics Packaging, Vol. 114, pp. 22-28.

Arvizu, D. and Moffat R.J., 1982, "The Use of Superposition in Calculating Cooling Requirements", Proceedings of the Electronics Cooling Conference IEEE, San Diego, CA, USA, pp. 133-144.

Arvizu, D., Ortega, A. and Moffat, R.J., 1985, In: Oktay, S. and Moffat R.J. (Eds.), "Cooling Electronic Components: Forced Convection Experiments with an Air-Cooled Array", Electronics Cooling, ASME, New York, USA.

Incropera, F.P., Kerby, J.S., Moffat, D.F. and Ramadhyani, S., 1986, "Convection Heat Transfer from Discrete Heat Sources in a Rectangular Channel", International Journal of Heat and Mass Transfer, Vol. 29, pp. 1051-1058.

Kays, W.M. and Crawford, M.E., 1993, "Convective Heat and Mass Transfer", 3rd ed., McGraw-Hill, New York, USA, 601p.

Mahaney, H.V., Incropera, F.P. and Ramadhyani, S., 1990, "Comparison of Predicted and Measured Mixed Convection Heat Transfer from an Array of Discrete Sources in a Horizontal Rectangular Channel", International Journal of Heat and Mass Transfer, Vol. 33, pp. 1233-1245.

Moffat, R.J., 1998, "What's New in Convective Heat Transfer?", International Journal of Heat and Fluid Flow, Vol. 19, pp. 90-101.

Moffat, R.J., 2004, "$h_{adiabatic}$ and u'_{max}", Journal of Electronics Packaging, Vol. 126, pp. 501-509.

Patankar, S.V., 1980, "Numerical Heat Transfer and Fluid Flow", Hemisphere Publishing Corporation, New York, USA, 197p.

Ortega, A. and Lall, B.S., 1992, "A Clarification of the Adiabatic Heat Transfer Coefficient as Applied to Convective Cooling of Electronics", Proceedings of the 8th Annual IEEE Semiconductor Thermal Measurement and Management Symposium, Austin, TX, USA, pp. 1-3.

Sugavanam, R., Ortega, A. and Choi, C.Y., 1995, "A Numerical Investigation of Conjugate Heat Transfer from a Flush Heat Source on a Conductive Board in Laminar Channel Flow", International Journal of Heat and Mass Transfer, Vol. 38, pp. 2969-2984.

7. RESPONSIBILITY NOTICE

The authors are the only responsible for the printed material included in this paper.